www.nature.com/sc

ISCoS The International Spinal Cord Society

ARTICLE

Analysis and comparison of a spinal cord injury model with a single-axle-lever clip or a parallel-moving clip compression in rats

Xiao-hui Wang[1,2,4], Chao Jiang[1,2,4], Yong-yuan Zhang[1,2], Zhe Chen[1,2], Zhi-yuan Wang[1,2], Hao Yang[1,3] and Ding-jun Hao[1,2]✉

STUDY DESIGN: Experimental animal study.
OBJECTIVES: To assess the feasibility of a custom-designed parallel-moving (PM) clip, compared with a single-axle-lever (SAL) clip, for the development of a compressional spinal cord injury (SCI) model in rats.
SETTING: Hospital laboratory in China.
METHODS: We used a PM clip and a SAL clip with same compression rate, to develop a SCI model in rats, and set a sham group as a blank control. Within 3 weeks, each group of rats was evaluated for behavioral (Basso–Beattie–Bresnahan locomotor rating score, BBB), and electrophysiological changes (somatosensory evoked potential), and historical staining to observe the differences between the three groups. In particular, the mechanical results of the PM group were calculated.
RESULTS: The BBB scores for the SAL and PM groups were significantly lower than those for the sham group ($P < 0.05$), no significant difference between the two methods ($P > 0.05$), but the values corresponding to the PM group had smaller standard deviations. The interpeak-latency (IPL) was significantly prolonged ($P < 0.0001$) and the peak-peak amplitude (PPA) was significantly reduced ($P < 0.01$) in SAL and PM groups than those in the sham group, but there was no statistical difference in both IPL and PPA between the two SCI groups ($P > 0.05$). Histological staining showed obvious pathological changes in two SCI groups, and the shape of the lesion zone in the PM group was more symmetrical than that in the SAL groups.
CONCLUSIONS: The use of a compressional SCI model in rats with the PM clip we designed is an appropriate method to quantify the injury. The degree of the injury caused by this clip is more stable and uniform than those with classical methods.

Spinal Cord (2022) 60:332–338; https://doi.org/10.1038/s41393-021-00720-7

INTRODUCTION

Spinal cord injury (SCI) is a severe and irreversible trauma to the central nervous system, which often results in partial or complete loss of sensory, motor, reflex, and autonomic nerve functions below the injured level [1]. SCI is often caused by falling and sport injuries, traffic accidents, and heavy objects, and it is difficult to recover the function after injury, causing huge social and economic burden [2, 3]. This type of trauma results in high disability and the available therapies are limited; therefore, it has become a hot topic in current medical research [4]. Due to the complex pathophysiological mechanism, the efficacy of neural function reconstruction after SCI is still poor. The use of animal models to study the mechanism of SCI in humans and its treatment is currently the main way of studying SCI.

The SCI model with clip compression in rats is an easy and highly reproducible animal model that mimics the pathophysiological process of acute SCI in the clinic, and it was first proposed and used by Rivlin in 1978 [5–7]. As in aneurysm clips or calibrated forceps, the mechanical mode of this tool is similar to a single-axle-lever structure that clips around the shaft and can control the extent of the damage by changing the pressure and time of clamping with low cost [8, 9].

The main problems of this type of SCI model are that the force applied during compression and the velocity of the clips cannot be assessed [10, 11]. Moreover, according to our schematic analysis of the forces exerted on the spinal cord by the clip during the compressing process (the red structure in Fig. 1a), we found that when we compress the spinal cords, the force is transmitted along the curve, and it is not applied completely in the direction of the maximum transverse diameter of the spinal cord. Therefore, the same operation may cause a difference in the injury extent due to the difference in the spinal cord width in experimental animals (Fig. 1b).

In this study, we designed a parallel-moving (PM) clip that was different from the traditional single-axle-lever-moving clip such as the aneurysm clip or calibrated forceps. The force of the compression and velocity of the clips can be evaluated through the force calculation equation of the lead screw based on the moving distance and time. Afterwards, behavioral, electrophysiology, and morphology were used to evaluate the quality of the

[1]Department of Orthopedic, the First Affiliated Hospital of Xi'an Jiaotong University, Xi'an 710061 Shaanxi, China. [2]Department of Spinal Surgery, Honghui Hospital, Xi'an Jiaotong University, Xi'an 710054 Shaanxi, China. [3]Translational Medicine Center, Honghui Hospital, Xi'an Jiaotong University, Xi'an 710054 Shaanxi, China. [4]These authors contributed equally: Xiao-hui Wang, Chao Jiang. ✉email: haodingjun@mail.xjtu.edu.cn

Received: 5 March 2021 Revised: 25 September 2021 Accepted: 28 September 2021
Published online: 9 October 2021

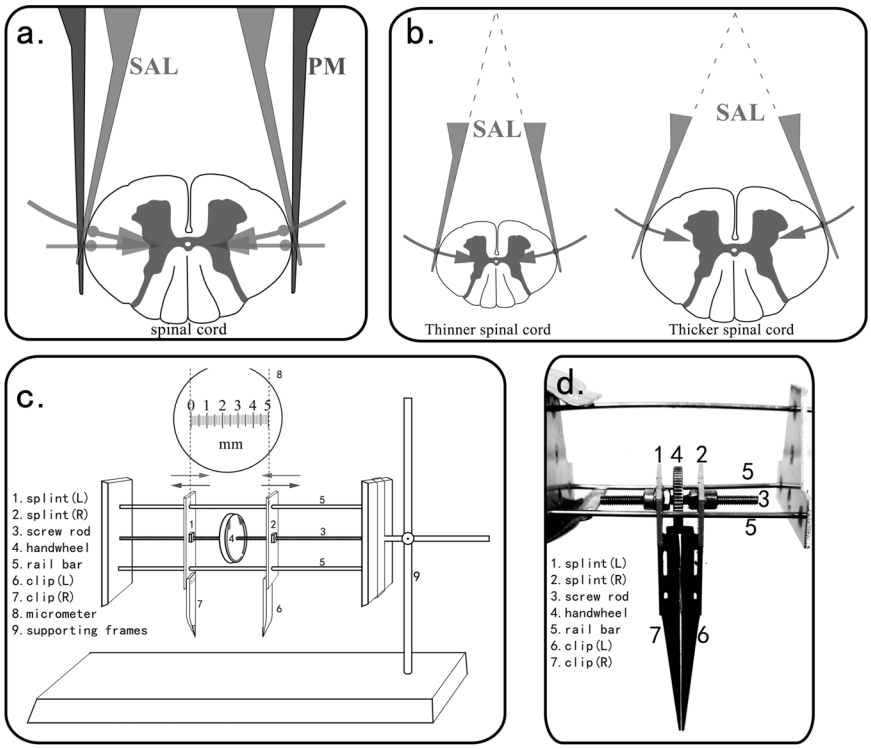

Fig. 1 Spinal cord clipping device. a Comparison of the point of action and pressure path of two kinds of spinal cord clipping. **b** Influence of spinal cord width on SCI in rat model with single-axle-lever clip compression. **c**, **d** The diagrammatic sketch of function and physical display of parallel-moving clamps.

model established with the two methods, and preliminarily confirmed the feasibility of the modified scheme to develop SCI rat models.

MATERIALS AND METHODS

Experimental animals and ethical statements

Healthy Sprague-Dawley (SD) rats (adult female, 2–3 months old, weighing 200–300 g) were used in the experiments to develop the SCI model and were provided by the Animal Feeding Center of the Xi'an Jiaotong University Health Science Center (Xi'an, SN, China). The rats were housed two per cage under room temperature (21 ± 1 °C), 50% humidity, and 12 h light/dark cycle with constant air renewal for 1 week before the experiment. The animals with SCI caused by the SAL clip or the custom-made PM clip were respectively abbreviated as SCI-SAL and SCI-PM groups hereinafter. Rats had free access to food and water. Twenty-one rats were randomly divided into three groups ($n = 7$): (I) SCI-SAL, animals with laminectomy, and SCI, through calibrated forceps; (II) SCI-PM, animals with laminectomy, and SCI with PM clip compression; and (III) sham, animals with laminectomy, without SCI. All experimental procedures were performed according to the Guide of Laboratory Animal Care and Use from the United States National Institutes of Health and were approved by the Institutional Animal Care and Use Committee (IACUC) of the Xi'an Jiaotong University.

Experimental procedures and quantitative methods

This section mainly describes the procedures for developing SCI animal models with PM clip compression designed by ourselves and the instructions for their use. PM clamps are mainly composed of a bracket, a guide rail, and a pair of splints that move in opposite directions (Fig. 1c, d). In brief, they convert the rotary motion of the handwheel into the horizontal linear motion of the splint through the lead screw system. A pair of clips connect the lower edge of each splint separately, the moving time is controllable, and the moving distance of the splints can be measured with an external micrometer.

Before using, the splint spacing was adjusted to the same width as the spinal cord; this is the initial distance, denoted as d_0. The tip of each clip was gently placed into the gap between the spinal cord and the canal (the blue structure in Fig. 1a), in contact but without compressing the spinal cord. According to the compression degree of the spinal cord required by the experiment, the handwheel was rotated to drive the splints to the final position. The micrometer was used to measure the splint spacing at that time, denoted as d_1. Therefore, the actual moving distance (denoted as l) of each splint is half of the moving distance ($d_0 - d_1$) minus the thickness of the handwheel (d_h):

$$l = \frac{(d_0 - d_1) - d_h}{2}$$

The lead of the screw thread connecting the handwheel and the splint of the PM clips is denoted as L, which is constant and represents the horizontal movement distance of the splint when the handwheel drives the screw to rotate 360° (the radius is 2π). When the splint moves the distance l in t_l seconds, the radius of the handwheel rotation is $2\pi l/L$. Therefore, under these conditions, the equation that relates the average angular acceleration (denoted as β) and the radius of the handwheel rotation is:

$$\int_0^{t_l} \frac{\beta}{2} dt^2 = \frac{2\pi l}{L}$$

The average angular acceleration β is:

$$\beta = \frac{4\pi l}{L t_l^2}$$

The total mass of the handwheel and screw is denoted as m, and the rotational inertia of the handwheel-screw system is s $J = m{\cdot}r^2$. Therefore, the torque of this motion, denoted as T, if the handwheel radius is r, is:

$$T = J \cdot \beta = \frac{4\pi m r^2 l}{L t_l^2}$$

According to the force transmission formula of the lead-screw [12], the compressional force (denoted as P) of one splint to the spinal cord can be obtained as follows:

$$P = \frac{2\pi\eta T}{L} = \frac{8\pi^2 m \eta r^2 l}{L^2 t_l^2}$$

For the same equipment, the transmission efficiency of the lead screw η, the radius of the handwheel r, the mass of the handwheel plus screw m, and the lead of the screw thread L, are fixed parameters and the variable is l/t_l^2. In addition, the speed of the clips can also be measured through the relationship between the moving distance and moving time.

$$v = l/t_l$$

Establishment of an SCI model in rats

The surgery for the SCI-SAL and sham groups were mainly performed as previously described [13, 14]. Twenty-four adult SD rats were randomly divided into three groups of eight animals. Rats in each group were anesthetized intraperitoneally with 1% sodium phenobarbital (40 mg/kg). After general anesthesia, the limbs were bound and fixed on the operating table, and Vaseline was used on the eyes to prevent drying during surgery. The skin overlying the T2–12 vertebrae was shaved, cleaned, and disinfected with 10% iodophor and 75% alcohol (Fig. 2a). A longitudinal incision was performed overlying the T7–11 area using operating scissors in a sterile environment. After subperiosteal dissection of paraspinal muscles, a laminectomy was performed to expose the spinal cord from T9 or T10 for all groups (Fig. 2b, c). In the SCI-SAL group, a compression-type lesion was produced using a calibrated compression method with microsurgical forceps (Yunkang, Jiangsu, China, 0.8-mm tip) for 30 s; it took 5 s from the initial to the compressed state (Fig. 2d) [13]. In the SCI-PM group, the clips contacted the spinal cord first, then the handwheel rotated at a constant speed for 5 s, and the clips gradually clamped. Once the final compressed state was reached, it was maintained for 25 s (Fig. 2e). The spinal cord of rats in both SCI groups was reduced to 25% of the initial width. The damage ratio for the SCI-SAL group was controlled through the gasket between the tip of the forceps, and the SCI-PM group was controlled by measuring the distance between two splints with a micrometer; the spinal cords of the sham group were not injured. Once the processing for each group was complete, the spinal cords were rinsed with sterile saline preheated at 37 °C to promote hemostasis and the incision was closed. After operation, two rats were placed randomly in each cage, and penicillin (104 U) and gentamicin (8×10^4 U) (Sigma, Missouri, USA) were administered to each rat subcutaneously for 3 days to prevent postoperative infection [15].

Basso–Beattie–Bresnahan locomotor rating score (BBB score)

The BBB scores for each group were recorded 1 h before surgery, and 1 h (anesthesia awakening), 3 d, 7 d, 14 d, and 21d after surgery. The BBB scores for each group were observed and recorded by two members of the experimental team who were not aware of the group allocation, and then averaged.

Somatosensory evoked potential (SEP) signal determination

The PowerLab DAQ device (8 channels, ADInstruments, Australia) and needle electrodes (customized, KEDOUBC, China) were used to stimulate, detect, amplify, and filter electrophysiological signatures. A stimulating electrode was placed in the gastrocnemius muscle of the peroneal nerve at the skin. and recording electrodes were placed in the motor cortex. The negative electrode was placed under the scalp, and the reference electrode was placed in the paravertebral muscle. The common peroneal nerve was stimulated through a continuous pulse, and the stimulation voltage was 3 V. The stimulator continued to stimulate the common peroneal nerve of the rats by sending square waves (bandwidth,1 ms; frequency, 10 Hz; filter frequency, 300 Hz; 300 times). When the stimulation intensity gradually increased 2–3 times above the motor threshold of rats, mild convulsion of the lower limb muscles was observed. The square wave SEPs were measured at 10 min, and on days 7, 14, and 21 after surgery. The wave form of N22-P40 SEP was superimposed and processed, then the IPL and the peak difference between P and N waves (PPA) were calculated. After the operation, the incision was closed and antibiotics were injected intramuscularly.

Histomorphological observations

Three rats per group were operated as previously indicated. The spinal cords were collected and stained on day 7 after surgery. Rats were anesthetized and perfused intracardially with 200 mL of phosphate buffered saline, pH 7.4, followed by 300 mL of 4% paraformaldehyde. Spinal cords were dissected and fixed in 4% paraformaldehyde at 4 °C overnight. The next day, tissues were cryoprotected in 30% sucrose for 48–72 h after, cut into segments of ~2 cm centered on the compression site, and embedded in embedding matrix (OCT, SAKURA, USA) at the appropriate temperature. Spinal cords were serially sectioned in the sagittal plane in 10-μm segments and attached to poly-L-lysine coated slides (Boster, China). All sections were obtained from a region at ~1 mm from the central sagittal plane, and were collected symmetrically. The specimen sections were stained with hematoxylin-eosin (H&E).

Statistical analyses

All numerical data conforming to a normal distribution were expressed as the mean ± standard deviation (SD). The comparison of multiple sample means was statistically assessed with ANOVA of repeated numerical data, and the pair comparison between multiple sample means was performed through t-test of paired sample means. The experimental data were analyzed using SPSS 22.0 (SPSS Inc, Chicago, IL, USA). The figures were made with GraphPad Prism7 (GraphPad Software, CA, USA). $P < 0.05$ was considered significantly different.

RESULTS

The general condition

The experimental animals were divided into three groups with eight animals per group for 3 weeks. In the sham group, no cases of SCI were observed and all the rats survived after operation. All the rats in the SCI-SAL and SCI-PM groups showed expected symptoms of SCI after surgery (loss of motor and sensory function in both lower limbs, dysuria, and dyspepsia). One animal in the SCI-SAL group and one in the SCI-PM group died due to postoperative infection. The success rate of the model was 87.25% in the SCI-SAL and SCI-PM groups. The number of animals in each group were compensated in time.

The mechanics of the SCI-PM group

In the SCI-PM group, one of the eight rats died on day 5 after surgery. The total mass of the handwheel and screw, m, was 4.25×10^{-3} kg. The transmission efficiency of the lead screw, η, was 60%. The handwheel radius, r, was 15 mm and the lead of the screw thread, L, was 0.3 mm. These indexes were substituted into the following equations to obtain the unilateral compressional force $P_1 - P_7$ and velocity of the compression on the spinal cord for each rat for 5 s.

$$P = \frac{8\pi^2 m\eta r^2 l}{L^2 t_l^2},\ v = l/t_l,\ Impulse = P/t_l$$

Behavioral characteristics

BBB scores for rats in each group changed over time as shown in Fig. 3a. The sham group had a transient lower limb movement disorder on the day of operation, recovered quickly within a few days, and the disorder started again 3 days later. No statistically significant difference in BBB scores at each record time (3, 7, 14, and 21 days) was observed in the sham group ($P > 0.05$) from day 3 after operation. Meanwhile, the scores of the SCI-SAL and SCI-PM groups were significantly lower than those of the sham group (SCI-SAL group vs. sham group, $t = 3.567$, $P < 0.05$; SCI-PM group vs. sham group, $t = 3.554$, $P < 0.05$). In this study, both models were successful from the perspective of the behavior after SCI, and there was no statistically significant difference between the two methods ($P > 0.05$). According to the detailed statistics, BBB scores (mean ± SD) were 3.57 ± 1.13 (day 14) and 6.14 ± 1.57 (day 21) in the SCI-PM group, and 6.71 ± 7.20 (day 14) and 9.29 ± 6.92 (day 21) in the SAL group. The scores for rats in the SCI-SAL group were more scattered based on the results of their SD range.

Electrophysiological results (SEP)

The IPL/PPA of rats in each group changed over time as shown in Fig. 3b, c. Compared with the sham group, the IPL was

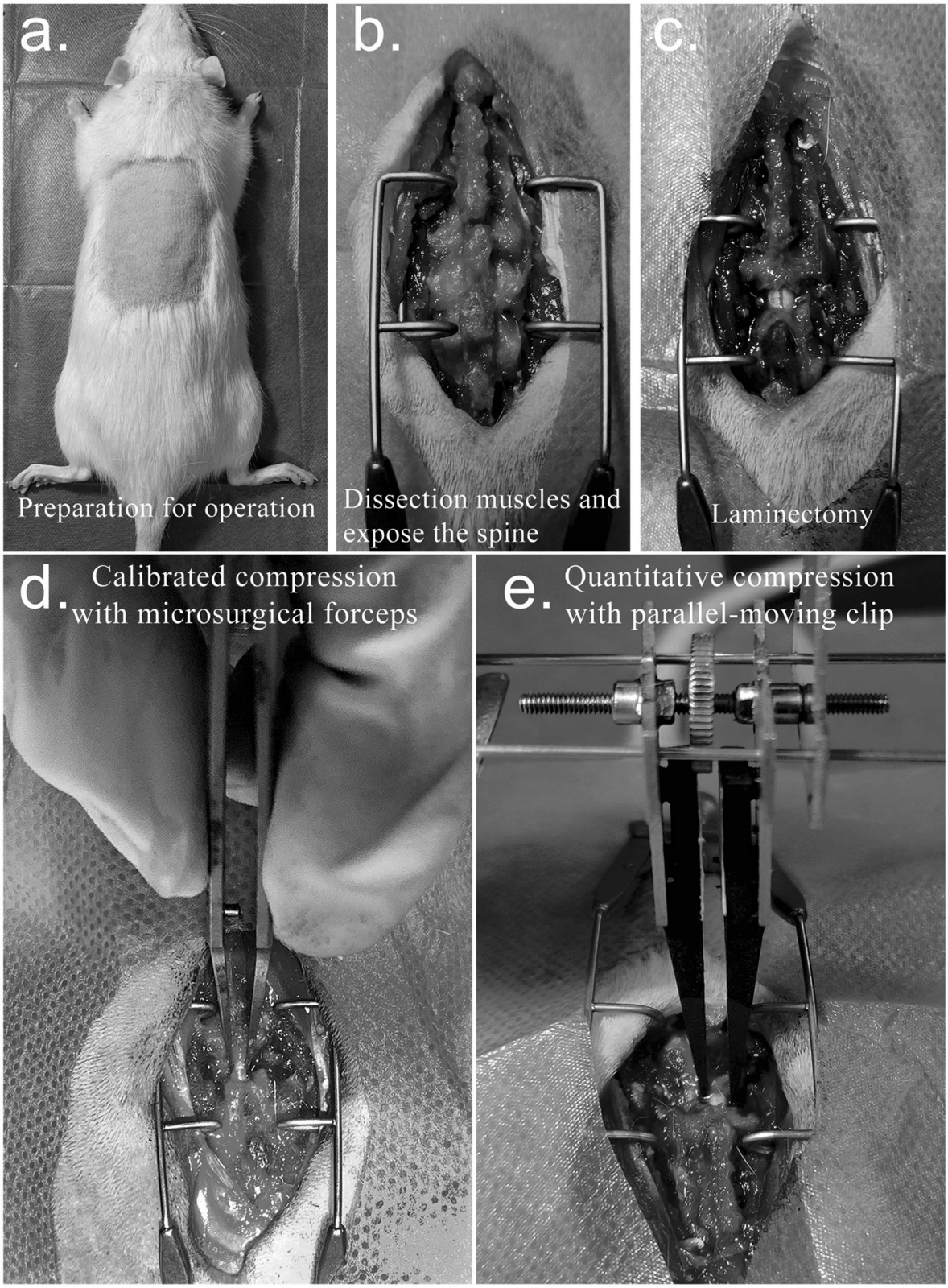

Fig. 2 Spinal cord clipping surgery was performed to establish SCI model with clip compression in rat. a Shaving and disinfection of the surgical area. **b** Subperiosteal dissection of paraspinal muscles, expose the vertebral lamina. **c** Laminectomy was performed to expose the spinal cord from T9. **d** Spinal cord injury caused by single-axle-lever clip. **e** Spinal cord injury caused by parallel-moving clip.

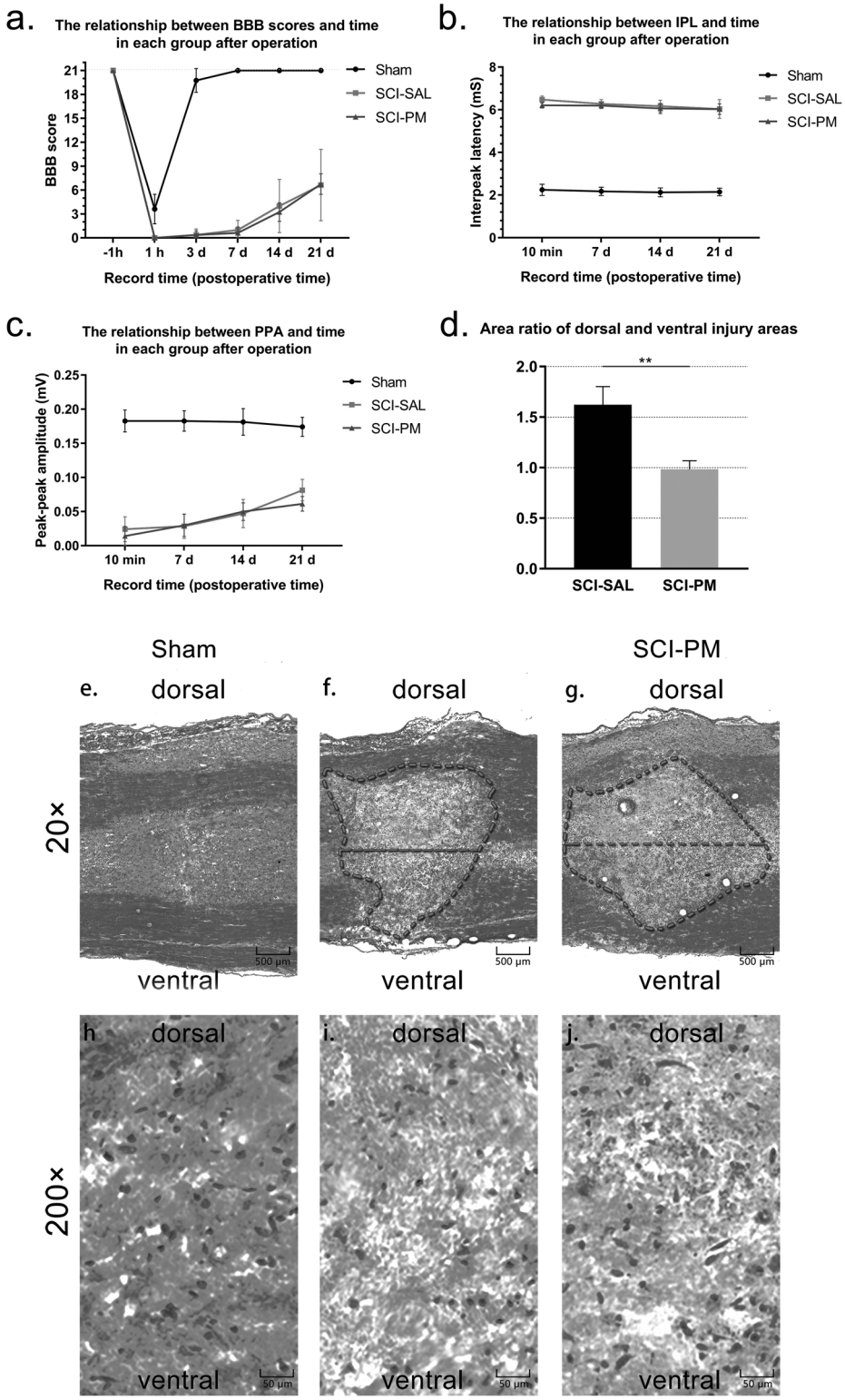

Fig. 3 Graphs of behavioral and electrophysiological data over time. a The relationship between BBB scores and time in each group after modeling operation. **b** The relationship between interpeak latency and time (IPL) of rats in each group after modeling operation. **c** The relationship between peak–peak amplitude (PPA) with time in rats of each group after modeling operation. **d** The area ratio of the dorsal and ventral injury areas, the injury area was segmented by the red median line between the upper to the lower boundary of the injury area such like in panels **f** and **g**. **e**–**j** H&E-stained sagittal section of the spinal cord showing the SCI. Representative images of in the gray matter at the lesion site or exposure site, nuclei are stained blue and cytoplasm is stained red ($n = 3$ per group; original magnification, ×20 and ×200).

significantly prolonged (SCI-SAL group vs. sham group, $t = 57.13$, $P < 0.0001$; SCI-PM group vs. sham group, $t = 134.7$, $P < 0.0001$) and the PPA was significantly reduced (SCI-SAL group vs. sham group, $t = 8.993$, $P < 0.01$; SCI-PM group vs. sham group, $t = 11.6$, $P < 0.01$) in the SCI-SAL and SCI-PM groups. However, no significant difference in IPL and PPA was found between the two experimental groups ($P > 0.05$).

H&E staining results

The H&E–stained sagittal section of the spinal cord shows the lesion site or exposure site of the spinal cord (Fig. 3e–j). Compared with the sham group (Fig. 3e, h), a dramatic loss of cells was detected in the injury center and significant edema of the gray matter following a compressional injury (Fig. 3f, g, i, j). Moreover, these aforementioned pathological changes in the gray matter were progressively aggravated from the ventral to dorsal spinal cord in the SCI-SAL group, while in the SCI-PM group, the region of the injury was more symmetrical (Fig. 3f, g). The SCI area was segmented by the median line between the upper to the lower boundary of the injury area, and the ratio of the dorsal and ventral injury areas was calculated. As shown in Fig. 3d, the ratio of the injury for the SCI-PM group was 0.985 ± 0.032, and that for the SCI-SAL group was 1.622 ± 0.068. The dorsal and ventral injury degrees caused by our improved equipment were almost the same (very close to 1.000), while the dorsal injuries caused by the classical method were more serious than the ventral injuries (SCI-SAL group vs. SCI-PM group, $t = 8.487$, $P < 0.05$).

DISCUSSION

The ideal SCI rat model should mimic the changes in the human spinal cord after SCI as much as possible, that is, the spinal cord should gradually show similar function loss and pathological changes after compressed by a force [16]. Therefore, the ideal SCI rat modeling surgery should be improved considering the following conditions: (1) the process should be simple and low-cost, produced quickly and in large quantities, with low mortality, and fewer complications after surgery; (2) the extent and duration of the spinal cord compression should be easily controlled; (3) the model should be applied to different animals and the injured spinal cord segment should be flexibly changed; (4) causation and symptoms should be consistent with the clinical observation, simulating the characteristics of human SCI [7].

The SCI animal modeling method with clip compression is widely used and can adjust the extent of the injury through time and compressional width. For example, aneurysm clip or forceps with calibrated gasket are usually used to crush the spinal cord and cause injury in the SCI model with clip compression [14, 17, 18]. However, these classical calibrations are indirect. The indicators that directly affect the extent of SCI, such as the clamping force, velocity, and impulse, cannot not be calculated [11, 13, 19]. To calculate the velocity of the force, thus to make the degree of spinal cord compression more accurate, we designed the PM clips, which are driven by a screw rod, and measured the total movement through the distance tool (Fig. 1c, d). Combined with the micrometer, the tool can measure the width of the spinal cord before compressing it, and determine the width of the compressed spinal cord according to the experimental settings. Then the model can achieve the final compressed state at a constant speed within a preset time. That is, the compressional force can be calculated through the time of rotation and the distance of the unilateral clip movement during that period. In turn, the compressional force can also be changed by controlling the time and distance of the movement. The process is derived from the force conduction equation of the lead-screw structure, and the final variables are time and moving distance of the unilateral clip. The limitations of the classical method of clip compression for SCI were improved to a certain extent. We recorded the moving time and distance of the clip in the rat model developed through this method; and then, we calculated the results using the equations (Table 1). The results agree well with the damage intensity in the SCI-SAL group according to the BBB score and electrophysiological results (Fig. 3a–c), but the compressional force, velocity, and impulse in the SCI-SAL group are not quantified with the classical tools due to their non-ideal single-axis-lever construction. In addition, it is worth noting that the BBB scores for the SCI-SAL group are more scattered than those of the SCI-PM group at 3, 7, 14, and 21 days after surgery, which also indicates that the SCI model of the SCI-PM group developed through the quantitative method is more stable (Fig. 3a). In addition, the BBB test reflects the locomotor behavior only. If the animal models developed through this method are to be used as a reference for SCI in humans, it will also require to measure more refined sensory-motor functions, which will need further behavior testing [20]. Compared with BBB scores, SEP is a quantitative and objective electrophysiological test, which can be used for the localization and quantitative analysis of SCI, and the degree of extension of IPL and reduction of PPA can be used to determine the severity of SCI [21]. From our results, the IPL of the experimental groups with the two methods were prolonged and their PPA were decreased, compared with those of the sham group, in agreement with the electrophysiological change after SCI.

Table 1. The mechanic results for the SCI-PM group.

	1	2	3	4	5	6	7
l_i (mm)	1.250	1.040	1.150	1.020	1.210	1.070	1.100
P_i (N)	0.042	0.034	0.038	0.034	0.040	0.036	0.036
v_i (mm/s)	0.250	0.208	0.230	0.204	0.242	0.214	0.220
Impulse ($\times 10^{-3}$ N/s)	8.40	6.80	7.60	6.80	8.00	7.20	7.20

The focus of this study was to design and test PM clips that can be used to develop SCI models in rats, and calculate the compressional force, velocity, and impulse during clip compression. In addition, we found that the lesion zone in the gray matter in the SCI-SAL group was approximately an inverted triangle (Fig. 3f). The lesion zone in the gray matter has an approximately uniform rhomboid shape in the SCI-PM group (Fig. 3g), although the pathological features are similar within the lesion area (Fig. 3i, j). In other words, compared with the SCI-PM group, the SCI-SAL group showed an "asymmetrical" lesion with the lesion in the dorsal side more severe than that of the ventral side (Fig. 3d). We hypothesized that this might be the case as shown in Fig. 1a, when the forceps with calibrated gasket is clamped to compress the spinal cord, and the contact surface between the forceps and spinal cord are closer to the dorsal side than the PM clips. In fact, the traumatic SCI usually caused by the failure of the spinal column (fracture and/or dislocation) directly imparts force to the spinal cord, disrupting axons, blood vessels, and cell membranes [22, 23]. Therefore, in most of the traumatic SCI clinically observed, the compression of the spinal cord is caused by the anterior burst or displaced vertebral body. Thus, in most clinical traumatic SCI situations, the ventral SCI should not be less severe than the dorsal spinal cord injury. From this point of view, the SCI model developed with PM clip compression is more consistent with the actual clinical pathological characteristics than that of the single-axle-lever clip compression. For basic research, the SCI model with clip compression, as a type of incomplete injury model, is more commonly used in the study of cell transplantation therapy or mechanisms of secondary injury [24]. Therefore, more precise and quantitative control of injury differences between individuals can reduce the errors in these basic studies. Our equipment provides such a solution.

CONCLUSIONS

The SCI models developed using the single-axle-lever clip and PM clip compression in rats achieved the simulation of SCI effectively. However, the quantification of the compressional force, velocity, and impulse to the spinal cord in the PM clip group is beyond the capability of those methods. In terms of the shape of the lesion zone, the results of the PM clip group were also more consistent with the clinical results, although this may need further evaluation. In summary, using the PM clips we designed, we developed a SCI model in rats that is more suitable for quantifying damage.

REFERENCES

1. Ramer LM, Ramer MS, Bradbury EJ. Restoring function after spinal cord injury: towards clinical translation of experimental strategies. Lancet Neurol. 2014;13:1241–56.
2. Kretzer, RM. A clinical perspective and definition of spinal cord injury. Spine (Phila Pa 1976). 2016;41:S27.
3. Cannon B. Sensation and loss. Nature. 2013;503:S2.
4. Liu D, Chen J, Jiang T, Li W, Huang Y, Lu X, et al. Biodegradable spheres protect traumatically injured spinal cord by alleviating the glutamate-induced excitotoxicity. Adv Mater. 2018;30:e1706032.
5. Rivlin AS, Tator CH. Effect of duration of acute spinal cord compression in a new acute cord injury model in the rat. Surgical Neurol. 1978;10:38–43.
6. Lv H, Yang J, Liao Z, Zhao Y, Huang Y. NG2 expression in rats with acute T (10) spinal cord injury. Neural Regen Res. 2012;05:41–44.
7. Cheriyan T, Ryan DJ, Weinreb JH, Cheriyan J, Paul JC, Lafage V, et al. Spinal cord injury models: a review. Spinal Cord 2014;52:588–95.
8. do Espírito Santo CC, da Silva Fiorin F, Ilha J, Duarte MMMF, Duarte T, Santos ARS. Spinal cord injury by clip-compression induces anxiety and depression-like behaviours in female rats: The role of the inflammatory response. Brain Behav Immun. 2019;78:91–104.
9. Chamankhah M, Eftekharpour E, Karimi-Abdolrezaee S, Boutros PC, San-Marina S, Fehlings MG. Genome-wide gene expression profiling of stress response in a spinal cord clip compression injury model. BMC Genomics. 2013;14:583.
10. Poon PC, Gupta D, Shoichet MS, Tator CH. Clip compression model is useful for thoracic spinal cord injuries: histologic and functional correlates. Spine (Phila Pa 1976). 2007;32:2853–9.
11. Abdullahi D, Annuar AA, Mohamad M, Aziz I, Sanusi J. Experimental spinal cord trauma: a review of mechanically induced spinal cord injury in rat models. Rev Neurosci 2017;28:15–20.
12. Ichikawa Y, Nishimoto T, Niwa K. TAILSTOCK CONTROL DEVICE, US20090199685[P]. 2009.
13. Vaughn CN, Iafrate JL, Henley JB, Stevenson EK, Shlifer IG, Jones TB. Cellular neuroinflammation in a lateral forceps compression model of spinal cord injury. Anat Rec (Hoboken). 2013;296:1229–46.
14. Khaing ZZ, Cates LN, DeWees DM, Hannah A, Mourad P, Bruce M, et al. Contrast-enhanced ultrasound to visualize hemodynamic changes after rodent spinal cord injury. J Neurosurg Spine. 2018;29:1–8.
15. Guo J, Cao G, Yang G, Zhang Y, Wang Y, Song W, et al. Transplantation of activated olfactory ensheathing cells by curcumin strengthens regeneration and recovery of function after spinal cord injury in rats. Cytotherapy. 2020;22:301–12.
16. Sharif-Alhoseini M, Khormali M, Rezaei M, Safdarian M, Hajighadery A, Khalatbari MM, et al. Animal models of spinal cord injury: a systematic review. Spinal Cord. 2017;55:714–21.
17. Rong H, Liu Y, Zhao Z, Feng J, Sun R, Ma Z, et al. Further Standardization in the Aneurysm Clip: The Effects of Occlusal Depth on the Outcome of Spinal Cord Injury in Rats. Spine. 2018;43:E126–E131.
18. McDonough A, Monterrubio A, Ariza J, Martínez-Cerdeño V. Calibrated forceps model of spinal cord compression injury. J Vis Exp. 2015;98:52318.
19. Plemel JR, Duncan G, Chen KW, Shannon C, Park S, Sparling JS, et al. A graded forceps crush spinal cord injury model in mice. J Neurotrauma. 2008;25:350–70.
20. Usmani S, Franceschi Biagioni A, Medelin M, Scaini D, Casani R, Aurand ER, et al. Functional rewiring across spinal injuries via biomimetic nanofiber scaffolds. Proc Natl Acad Sci USA. 2020;117:25212–8.
21. Agrawal G, Kerr C, Thakor NV, All AH. Characterization of graded mascis contusion spinal cord injury using somatosensory evoked potentials. Spine. 2010;35:1122–7.
22. Rowland JW, Hawryluk GW, Kwon B, Fehlings MG. Current status of acute spinal cord injury pathophysiology and emerging therapies: promise on the horizon. Neurosurg Focus. 2008;25:E2.
23. Denis F. The three column spine and its significance in the classification of acute thoracolumbar spinal injuries. Spine. 1983;8:817–31.
24. Ahmed RU, Alam M, Zheng YP. Experimental spinal cord injury and behavioral tests in laboratory rats. Heliyon. 2019;5:e01324.

ACKNOWLEDGEMENTS

The authors thank AiMi Academic Services (www.aimieditor.com) for the English language editing and review services.

AUTHOR CONTRIBUTIONS

XHW was responsible for designing the protocol, writing the protocol, design the device for surgery, participate in experimental operation, evaluating and writing the article; CJ was responsible for improving the experimental ideas and writing the protocol, participate in experimental operation in each tests, result collection and result analysis; YYZ and ZC guiding the modeling surgery, screening potentially eligible studies; ZYW assisted in the operation, recording partial postoperative indicators; HY help us solving some technical problems encountered; DJH providing financial support.

FUNDING

This work was supported by the National Natural Science Foundation of China (81830077).

COMPETING INTERESTS

The authors declare no competing interests.

ETHICAL APPROVAL

We certify that all experimental procedures were performed in accordance with the Guide of Laboratory Animal Care and Use from the United States National Institution of Health and were approved by the Institutional Animal Care and Use Committee (IACUC) of Xi'an Jiaotong University, SN, China.

ADDITIONAL INFORMATION

Correspondence and requests for materials should be addressed to Ding-jun Hao.